한국동력기계공학회지 제19권 제4호 pp. 89-96, 2015년 8월, ISSN 1226-7813(Print) ISSN 2384-1354(Online)
Journal of the Korean Society for Power System Engineering http://dx.doi.org/10.9726/kspse.2015.19.4.089
Vol. 19, No. 4, pp. 89-96, August 2015

Improvement of Conventional Sliding Mode Observer for Full Range Sensorless Control of a PMSM

Wahyu Kunto Wibowo* and Seok-Kwon Jeong*†

(Received 13 May 2015, Revision received 13 August 2015, Accepted 13 August 2015)

Abstract: This paper investigates some strategies to overcome the chattering problem of the conventional sliding mode observer (SMO) and to improve the rotor position estimation performance for full range sensorless control of a PMSM. An adaptive observer gain based on the Lyapunov's stability criterion and a cascade low pass filter with advanced phase delay compensation were proposed to reduce the chattering problem and to strengthen the filtering capability of the SMO. Several cases studies through experiments were carried out to confirm conventional SMO's problems and effectiveness of the proposed strategies. The experimental results show that the proposed method gives precise estimation on speed and rotor position when the motor rotates on 2% of its rated speed.

Key Words : Permanent magnet synchronous motor, Sensorless control, Adaptive observer gain, Cascade low pass filter, Sliding mode observer, Phase delay compensation

1. Introduction

The sensorless control, also called encoderless control, has been developing rapidly by many researchers to overcome the mechanical sensor disadvantages. There are two main categories of the sensorless control for PMSMs: signal injection and model based method. The signal injection method exploits the magnetic saliency of the machine to detect the electrical rotor position. This method offers a proper solution for standstill and low speed operation[1-3]. However, all of the latest works that adopted the signal injection method have some drawbacks. The injected signal causes noise to the system which makes degradation to the control performance and the system will fail to work in certain threshold speed. Furthermore, this method will not properly work on a surface mounted type PMSM because of its non-saliency characteristic. On the contrary, the model based method does not have those drawbacks. The model based method exploits a dynamic model of the motor to obtain the back electromotive force (EMF) or flux linkage. Afterwards, the electrical rotor position and speed information are estimated by using the back EMF. However, this method is only suited for medium to high speed operational range

*† Seok-Kwon Jeong(corresponding author) : Department of Refrigeration and Air-Conditioning, Pukyong National University.
E-mail : skjeong@pknu.ac.kr, Tel : 051-629-6181
*Wahyu Kunto Wibowo : Department of Mechatronics Engineering, Graduate School, Pukyong National University.

because the measured back EMF was too small at the low speed operation. Furthermore, the model based method is sensitive to the variation of motor parameter because it depends on a mathematical motor model[4,5].

In contrast with others observer of the model based method, the sliding mode observer (SMO) has better advantages comparing to other model based observer types. The SMO has attractive features such as mathematically easy to design and strong robustness regarding disturbance, parameter variation, and noise[6-10]. The estimation results of the speed and electrical rotor position based on the SMO were satisfactory at the medium to high speed operation. Chattering problem caused by the switching function has been remained as the main drawback of the SMO approach. This chattering will be magnified by the constant observer gain of the SMO which makes the estimation results deteriorated especially at the low speed operation. A low pass filter (LPF) usually takes place in the SMO to reduce the chattering problem. However, the LPF without proper cut-off frequency and phase delay compensation will cause the filter unable to suppress the chattering problem and cause a big phase delay on the rotor position estimation results. Hence, the estimation performance significantly declines when the PMSM rotates at the low speed range.

This paper investigates the conventional SMO's estimation performance at the low to high speed operation on the PMSM driven by the field oriented vector control in detail. The effect of the constant observer gain which could magnify the chattering problem and filtering performance of a LPF are inspected. Finally, this paper proposes an adaptive observer gain and a cascade low pass filter (CLPF) with advanced phase delay compensation to overcome the conventional SMO problems. The CLPF with advanced phase delay compensation is proposed to strengthen the filtering capability and compensate the phase delay of the estimated rotor position precisely for wide speed range sensorless control with lowering the threshold speed as shown in Fig. 1.

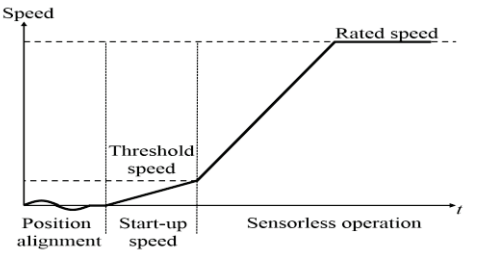

Fig. 1 Conceptual diagram of sensorless control

The proposed SMO estimation is implemented on a 32-bit fixed point digital signal processor (DSP). Several experiments are performed to check and to investigate the proposed SMO for the PMSM. The experimental results validate the effectiveness of the proposed strategies which applied at the low to high speed operation.

2. Mathematical model of a PMSM

A surfaced mounted PMSM is considered in this paper which its quadrature axis synchronous inductance of the motor equals to direct axis inductance ($L_d = L_q = L_s$). The voltage model of the surface mounted PMSM in $\alpha\beta$ stationary reference frame is shown as follows:

$$\begin{bmatrix} v_\alpha \\ v_\beta \end{bmatrix} = \begin{bmatrix} R_s + pL_s & 0 \\ 0 & R_s + pL_s \end{bmatrix} \begin{bmatrix} i_\alpha \\ i_\beta \end{bmatrix} + \begin{bmatrix} e_\alpha \\ e_\beta \end{bmatrix} \quad (1)$$

$$\begin{bmatrix} e_\alpha \\ e_\beta \end{bmatrix} = \omega_r \psi_r \begin{bmatrix} -sin\theta_r \\ cos\theta_r \end{bmatrix} \quad (2)$$

where $v_\alpha, v_\beta, i_\alpha$, and i_β are the stator voltages

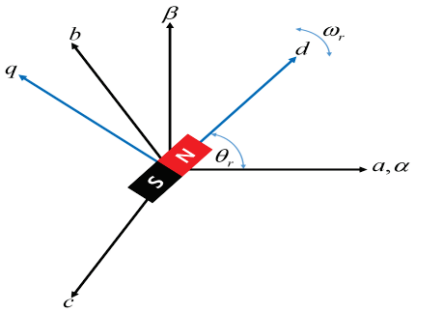

Fig. 2 Coordinates for mathematical model

and currents in stationary reference frame. R_s and L_s are the stator resistance and inductance respectively. ω_r and ψ_r represent the rotor angular speed and flux linkage generated by the rotor magnet. Notation p is the derivative of time. e_α and e_β are back EMF in $\alpha\beta$ stationary reference frame. Symbol θ_r represents the position of the rotor flux as shown in Fig. 2. Current model of the PMSM shown in Eq. (3) can be derived from Eq. (1) and Eq. (2).

$$\begin{bmatrix} pi_\alpha \\ pi_\beta \end{bmatrix} = -\frac{R_s}{L_s}\begin{bmatrix} i_\alpha \\ i_\beta \end{bmatrix} + \frac{1}{L_s}\begin{bmatrix} v_\alpha \\ v_\beta \end{bmatrix} - \frac{1}{L_s}\begin{bmatrix} e_\alpha \\ e_\beta \end{bmatrix} \tag{3}$$

3. Design of the sliding mode observer

3.1 Design of the SMO for speed estimation

The SMO is utilized in the system as a replacement of the physical sensor to obtain the rotor flux position and speed information. Eq. (3) is used to design the current observer as shown in Eq. (4). It is noted that all motor parameters are assumed as a constant.

$$\begin{bmatrix} p\hat{i}_\alpha \\ p\hat{i}_\beta \end{bmatrix} = -\frac{R_s}{L_s}\begin{bmatrix} \hat{i}_\alpha \\ \hat{i}_\beta \end{bmatrix} + \frac{1}{L_s}\begin{bmatrix} v_\alpha \\ v_\beta \end{bmatrix} - \frac{1}{L_s}\begin{bmatrix} z_\alpha \\ z_\beta \end{bmatrix} \tag{4}$$

$$\begin{bmatrix} z_\alpha \\ z_\beta \end{bmatrix} = K\begin{bmatrix} sign(\hat{i}_\alpha - i_\alpha) \\ sign(\hat{i}_\beta - i_\beta) \end{bmatrix} \tag{5}$$

Where the symbol hat "^" denotes the estimated value. K is the constant observer gain and symbol z is the switching signal which contains the estimated back EMF information. Dynamic estimation error can be obtained by subtracting Eq. (3) from Eq. (4):

$$\begin{bmatrix} p\bar{i}_\alpha \\ p\bar{i}_\beta \end{bmatrix} = -\frac{R_s}{L_s}\begin{bmatrix} \bar{i}_\alpha \\ \bar{i}_\beta \end{bmatrix} + \frac{1}{L_s}\begin{bmatrix} e_\alpha \\ e_\beta \end{bmatrix} - \frac{1}{L_s}\begin{bmatrix} z_\alpha \\ z_\beta \end{bmatrix} \tag{6}$$

where the symbol bar, "-", represents estimation error of each corresponding variable. The sliding surface is selected as:

$$S = \hat{i}_s - i_s \tag{7}$$

where $i_s = [i_\alpha \quad i_\beta]^T$ is the actual value and $\hat{i}_s = [\hat{i}_\alpha \quad \hat{i}_\beta]^T$ is the estimated value. Superscript T denotes transpose of a vector. When the estimated current reaches the sliding surface ($S = 0$), then the estimation error becomes zero and the estimated current tracks the actual value. Hence, $\hat{i}_s = i_s$, Eq. (6) will give:

$$[e_\alpha \quad e_\beta]^T = Ksign(\bar{i}_s). \tag{8}$$

The signum function was used in the conventional SMO as shown in Eq. (8). Currently, there are several options for the SMO to estimate the back EMF by using the discontinuous control functions such as signum, saturation, and sigmoid. However, the usage of those functions induce chattering problem. First order LPF is taking a place in the algorithm to minimize the chattering problem as represented in Eq. (9).

$$[\hat{e}_\alpha \quad \hat{e}_\beta]^T = \frac{\omega_c}{s + \omega_c}[z_\alpha \quad z_\beta]^T \tag{9}$$

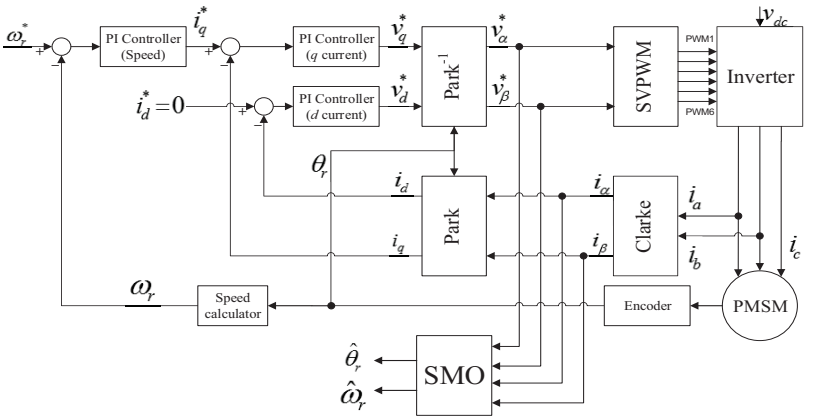

Fig. 3 Block diagram of a PMSM vector control with the SMO

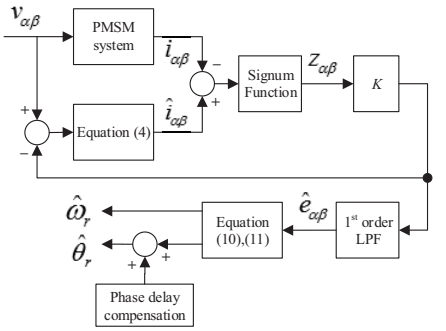

Fig. 4 The SMO with signum function

Where ω_c is the angular speed of the LPF which contains cut-off frequency f_c. The estimated back EMF results are directly used to calculate the rotor flux position and speed estimation as described in Eq. (10) and Eq. (11).

$$\hat{\theta}_r = -\tan^{-1}\frac{\hat{e}_\alpha}{\hat{e}_\beta} \tag{10}$$

$$\hat{\omega}_r = \frac{d\hat{\theta}_r}{dt} \tag{11}$$

Fig. 3 shows the block diagram of the field oriented vector control with the SMO for a PMSM. Fig. 4 shows the block diagram of the conventional SMO for a PMSM system.

3.2 The adaptive observer gain for a SMO

In this paper, an adaptive observer gain is proposed to overcome the problem of the constant gain observer on the SMO. The adaptive observer gain is designed through the Lyapunov stability criterion. The sliding surface described in Eq. (7) is defined as the estimation error of the stator current. When the condition $\dot{S}S < 0$ is satisfied, the sliding mode exists, and this implies that $S \to 0$ for $t \to \infty$, $S_\alpha = \bar{i}_\alpha$, and $S_\beta = \bar{i}_\beta$. The Lyapunov function candidate is defined in Eq. (12) to design the adaptive observer gain and to set up the stability condition of the SMO.

$$V = \frac{1}{2}S^T S = \frac{1}{2}\bar{i}_\alpha^2 + \bar{i}_\beta^2 \tag{12}$$

From the Lyapunov stability theorem, the system is asymptotically stable when $\dot{V} < 0$, hence:

$$\dot{V} = p\bar{i}_\alpha\bar{i}_\alpha + p\bar{i}_\beta\bar{i}_\beta. \tag{13}$$

The Lyapunov stability condition is satisfied as shown in Eq. (14) after by substituting Eq. (6) into Eq. (13).

$$K > max\left(|e_\alpha|, |e_\beta|\right) \tag{14}$$

The K represented in Eq. (14) is used in the conventional SMO as a constant value. The design of the adaptive observer gain in this paper is achieved by a simple addition from the Lyapunov's stability method that had already done until Eq. (14). The adaptive observer gain shown in Eq. (15) is designed based on Eq. (14) and Eq. (2). The back EMF, which described in Eq. (2), will reach the maximum value when the values of $sin\,\theta_r$ and $cos\,\theta_r$ are equal to 1. Hence, the adaptive observer gain of Eq. (15) can be obtained by substituting Eq. (2) into Eq. (14).

$$K = \omega_r^* \psi_r \tag{15}$$

Where ω_r^* is speed reference. With this adaptive method, the observer gain can adjust to the actual back EMF so that the gain is enough to estimate the back EMF precisely and able to suppress the chattering problem.

3.3 The cascade LPF with advanced phase delay compensation

A second order cascade LPF with advanced phase delay compensation method is proposed in this paper to strengthen the filtering capability instead of the first order LPF. The attenuation performance for suppressing the chattering problem will increase twice higher by using the cascade LPF. However, the usage of this filter causes a longer time delay in estimating the position of the rotor flux. The advanced phase delay compensation method is used to compensate the phase delay ($\Delta\theta$) precisely based on the given speed reference. Eq. (16) and Eq. (17) describe the proposed second order cascade LPF and its phase delay equation.

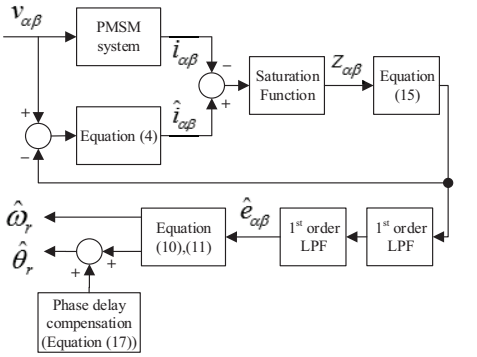

Fig. 5 The proposed SMO with saturation function

$$LPF_{2nd} = \frac{\omega_c^2}{s^2 + 2\omega_c s + \omega_c^2} \tag{16}$$

$$\Delta\theta = tan^{-1}\frac{2\hat{\omega}_r\omega_c}{\omega_c^2 - \hat{\omega}_r^2} \tag{17}$$

Appropriate cut-off frequency based on the speed reference is needed for the LPF in order to properly filtering the chattering problem and to accurately estimate the rotor flux position information for the variable control of PMSM applications. The cut-off frequency of the proposed cascade LPF and its phase delay are varied based on the given speed reference. Decision of the cut-off frequency f_c is described as follows:

$$f_c = \frac{nP}{120}. \tag{18}$$

Hence, the angular speed ω_c of the proposed second order cascade LPF with advanced phase delay compensation can be obtained in Eq. (19).

$$\omega_c = 2\pi\,\frac{nP}{120} \tag{19}$$

Fig. 5 shows the block diagram of the proposed SMO with a saturation function.

4. Experimental results and analysis

Some experiments were carried out to validate the proposed SMO. The experimental setup is shown in Fig. 6 and motor parameters are shown in Table 1. A 32-bit fixed point DSP is used to implement the proposed method. The sampling period of the control system is set at 100 μs.

Same speed profile and PI gains have been applied for two representative cases to compare and to investigate the results. The speed profile is applied in a stepwise, starts from 1000 rpm, then reduces to 500 rpm, and finally reduces to 40 rpm (2% of the rated speed).

Case 1: In this experiments, the conventional SMO with signum function shown in Fig. 2 was used as the speed and rotor flux position estimation method. The observer gain K and the

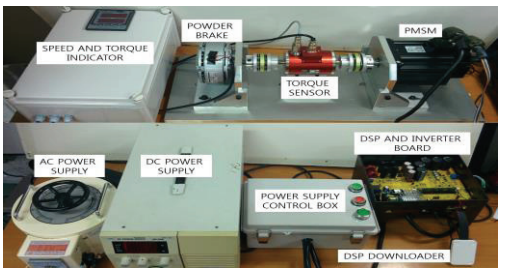

Fig. 6 The experimental system

Table 1 Parameters of the PMSM

Parameter (symbol)	Value (unit)
Rated power(P_r)	1.5 (kW)
Rated torque(T_e)	7.16 (N.m)
Rated speed(n)	2000 (rpm)
Stator resistance(R_s)	0.4 (Ω)
Stator inductance(L_s)	4.9×10^{-3} (H)
Flux linkage(ψ_r)	0.145 (Wb)
Inertia(J)	1.45×10^{-3} (Kg.m^2)
Pole number(P)	8

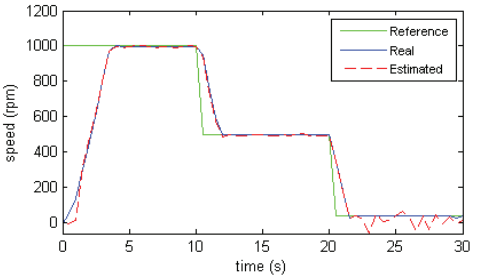

(a) speed responses

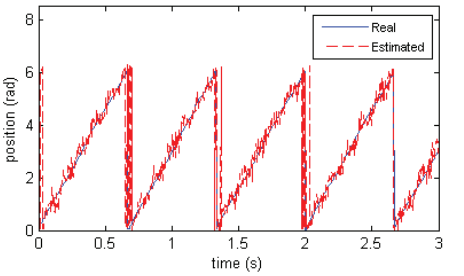

(b) rotor flux position at 40 rpm

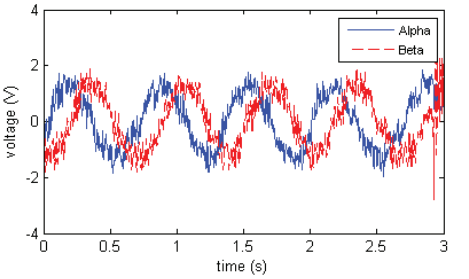

(c) back EMF estimation at 40 rpm

Fig. 7 Experimental results for case 1

cut-off frequency f_c of the LPF were set to a constant value based on the maximum rated speed of the motor, where $K = 105$ and $f_c = 133.33\,Hz$. Fig. 7 shows the experimental results for the case 1.

From the speed response shown in Fig. 7(a), the estimated speed could track the real speed with 2% steady state error at 1000 rpm and 500 rpm. However, the estimation became worst when the given speed reference is 40 rpm. The steady state error of the speed estimation was 190% from the speed reference at this low speed operation. From Fig. 7(b), the rotor flux position

estimation results at 40 rpm suffered a big error because of the chattering problem. The chattering problem was firstly appeared at the back EMF estimation shown in Fig. 7(c). The first order LPF was not able to suppress the chattering problem perfectly. The attenuation rate of the first order LPF was not sufficient to suppress the chattering problem. The first order LPF was failed to decrease the chattering problem because of the chattering mostly appeared in the lower frequency than the set cut-off frequency of the first order LPF. Moreover, the usage of a constant value cut-off frequency made a big phase delay on the rotor flux position estimation. Based on Fig. 7, this is why the conventional SMO was only preferred for the medium to high speed operation, because the constant values of the observer gain K and the cut-off frequency f_c were not suitable for the low speed estimation. The chattering in the estimated back EMF was magnified maximally by the constant observer gain and the LPF was failed to minimize the chattering when the motor operated at the low speed area.

Case 2: In this experiment, the proposed SMO as shown in Fig. 5 was examined to check the effectiveness of the proposed method. The proposed adaptive observer gain and second order cascade LPF with advanced phase delay compensation were used in order to minimize the chattering problem and to increase the filtering performance simultaneously.

The experimental result in Fig. 8 shows the proposed system responses. The estimated speed and rotor flux position results as shown in Fig. 8(a) and Fig. 8(b) were precisely tracking the real values. The steady state error of the estimated speed was below 0.5% at the medium to high

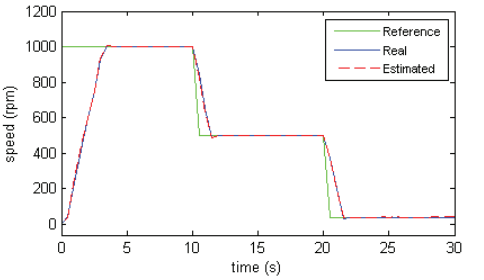

(a) speed responses

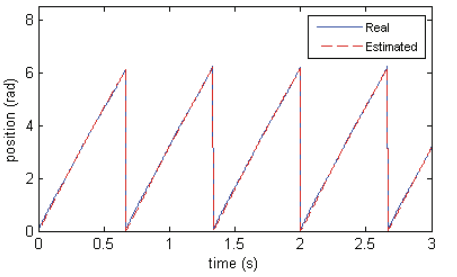

(b) rotor flux position at 40 rpm

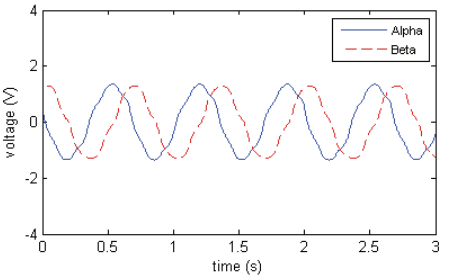

(c) back EMF estimation at 40 rpm

Fig. 8 Experimental results for case 2

speed and 2.5% at the low speed operation. The chattering which happened in the back EMF was decreased minimally as shown in Fig. 8(c), hence the rotor flux position was precisely estimated. Furthermore, the usage of the proposed second order cascade LPF with advanced phase delay compensation method was able to minimize the phase delay. From this experimental results, it is clear that the proposed SMO was able to estimate the speed and the rotor flux position precisely in the wide speed range.

The proposed SMO shows good improvement and strong robustness in estimation performance

especially at the low speed operation. Hence, this proposed estimation strategy will contribute to precise sensorless control of a PMSM over full speed range.

5. Conclusions

This paper proposed a strategy to improve the estimation precision for a PMSM with SMO. The adaptive observer gain and second order cascade LPF with advanced phase delay compensation were proposed in order to escalate and to expand the operation range of the SMO. Experimental results indicate that the speed and rotor flux position were precisely estimated by the proposed SMO. The adaptive observer gain effectively suppressed the chattering problem. The second order cascade LPF with advanced phase delay compensation successfully reduced the chattering problem and precisely compensated the phase delay of the estimated rotor flux position. The experimental results implied that the proposed SMO has strong robustness under extreme parameter variation. Moreover, the estimation performance was improved especially at the low speed operation by applying the proposed SMO.

Acknowledgement

This work was supported by a Research Grant of Pukyong National University (2014 year):

References

1. A. Accetta, M. Cirrincione, and M. Pucci, “TLS EXIN based neural sensorless control of a high dynamic PMSM,” *Control Eng. Pract.*, Vol. 20, No. 7, pp. 725–732, Jul. 2012.
2. Z. Q. Zhu and L. M. Gong, “Investigation of Effectiveness of Sensorless Operation in Carrier Signal Injection Based Sensorless-Control Methods,” *IEEE Trans. Ind. Electron.*, Vol. 58, No. 8, pp. 3431–3439, Aug. 2011.
3. F. Cupertino, G. Pellegrino, P. Giangrande, S. Member, and L. Salvatore, “Sensorless Position Control of Permanent-Magnet Motors With Pulsating Current Injection and Compensation of Motor End Effects,” *IEEE Trans. Ind. Appl.*, Vol. 47, No. 3, pp. 1371–1379, 2011.
4. P. Brandstetter, P. Rech, and P. Simonik, “Sensorless Control of Permanent Magnet Synchronous Motor Using Luenberger Observer,” in *Progress in Electromagnetics Research Symposium Proceedings,* pp. 424–428, 2010.
5. D. Xu, S. Zhang, and J. Liu, “Very-low speed control of PMSM based on EKF estimation with closed loop optimized parameters.,” *ISA Trans.*, Vol. 52, No. 6, pp. 835–43, Nov. 2013.
6. W. C. Chi and M. Y. Cheng, “Implementation of a sliding-mode-based position sensorless drive for high-speed micro permanent-magnet synchronous motors.,” *ISA Trans.*, Vol. 53, No. 2, pp. 444–53, Mar. 2014.
7. J. J. Ren, Y. C. Liu, N. Wang, and S. Y. Liu, “Sensorless control of ship propulsion interior permanent magnet synchronous motor based on a new sliding mode observer.,” *ISA Trans.*, pp. 1–12, Sep. 2014.
8. Y. Zhao, W. Qiao, and L. Wu, “Compensation Algorithms for Sliding Mode Observers in Sensorless Control of IPMSMs Compensation Algorithms for Sliding Mode Observers in Sensorless Control of IPMSMs,” *Fac. Publ. from Dep. Electr. Eng.*, 2012.
9. Y. S. Kung, V. Q. Nguyen, C. C. Huang, and L. C. Huang, “Simulink/ModelSim co-simulation of sensorless PMSM speed controller,” in *IEEE Symposium on Industrial Electronics and Applications*, 2011, No. 2, pp. 24–29.
10. Y. Jung and M. Kim, “Sliding Mode Observer for Sensorless Control of IPMSM Drives,” *J. Power Electron.*, Vol. 9, No. 1, pp. 117–123, 2009.